J. Geophys. 44, 603 – 612, 1978

Journal of Geophysics

The Reflectivity Method for a Buried Source

R. Kind

Seismologisches Zentralobservatorium, Krankenhausstr. 1–3, D-8520 Erlangen, Federal Republic of Germany

Abstract. The reflectivity method for the computation of theoretical seismograms is extended for the case of a point source buried in a layered medium. Two sources are considered, an explosive source and a vertical single force. Appearing accuracy problems are solved. Poles of Rayleigh waves are shifted away from the real axis of the wavenumber plane by introducing attenuation, in order to allow numerical integration along the real axis. The results of several computations are discussed. This method allows the computation of complete seismograms including surface waves, leaking modes and all body wave phases, including depth phases like *pP*.

Key words: Theoretical seismograms – Buried source – Thomson-Haskell matrix formalism.

Introduction

The reflectivity method of Fuchs (1968) computes theoretical seismograms for the case of an explosive point source located in a half-space on top of a layered medium. The essential points in this method are the numerical integration over the wavenumber and the application of the Thomson-Haskell matrix formalism. This method has been used extensively in various fields of seismology. It computes complete theoretical seismograms, of course only for the model, for which it was derived. Surface waves and body wave phases, which are due to the depth of the focus in the earth are not computed by this original version of the reflectivity method. The problem of the computation of the displacement at the free surface due to a source buried in a layered medium was solved analytically by Harkrider (1964). In the present paper a method is described, which applies numerical integration to Harkrider's analytical solution. The same accuracy problem, which is well known from the Thomson-Haskell formalism and which was solved by the delta matrix extension (Dunkin, 1965), also appears in the present numerical method. A solution of this problem is given. The numerical

0340-062X/78/0044/0603/$02.00

integration is carried out along the real axis in a finite wavenumber window. Rayleigh poles are shifted away from the real axis by the introduction of attenuation. Therefore, theoretical seismograms computed by this method always include the influence of attenuation.

Method

Details of the analytical derivation are given by Harkrider (1964). His results are summarized in the following. He derives the horizontal and vertical surface displacements, u_0 and w_0, for the case of a layered medium from the matrix equation

$$\begin{pmatrix} \Delta_n \\ \Delta_n \\ \omega_n \\ \omega_n \end{pmatrix} = J \left[\begin{pmatrix} \dot{u}_0/c \\ \dot{w}_0/c \\ 0 \\ 0 \end{pmatrix} + A^{-1} \begin{pmatrix} \Delta_1 \\ \Delta_2 \\ \Delta_3 \\ \Delta_4 \end{pmatrix} \right], \tag{1}$$

where Δ_n and ω_n are the potential coefficients for *P-SV* waves in the half-space, J is the product of the Haskell matrices (Haskell, 1953) of the half-space and of all layers. A is the product of the Haskell matrices of all layers above the source, and $(\Delta_1, \Delta_2, \Delta_3, \Delta_4)$ is the discontinuous displacement-stress source vector. The homogeneous source layer is divided into two layers at the source level. Only the part of the source layer above the source is contained in A. Rewriting (1) in the form

$$\begin{pmatrix} \Delta_n \\ \Delta_n \\ \omega_n \\ \omega_n \end{pmatrix} = J \begin{pmatrix} W \\ X \\ Y \\ Z \end{pmatrix}$$

and solving for $\dot{u}_0/c$ and $\dot{w}_0/c$ yields (see Harkrider 1964, 1970)

$$\dot{u}_0/c = W - (A_{44}\Delta_1 - A_{34}\Delta_2 + A_{24}\Delta_3 - A_{14}\Delta_4)$$

$$\dot{w}_0/c = X - (-A_{43}\Delta_1 + A_{33}\Delta_2 - A_{23}\Delta_3 + A_{13}\Delta_4)$$

with

$$X = \frac{R_{12}Y + R_{13}Z}{-R_{11}}$$

$$W = \frac{R_{14}Y + R_{15}Z}{R_{11}}$$

and

$$Y = A_{42}\Delta_1 - A_{32}\Delta_2 + A_{22}\Delta_3 - A_{12}\Delta_4$$

$$Z = -A_{41}\Delta_1 + A_{31}\Delta_2 - A_{21}\Delta_3 + A_{11}\Delta_4.$$

The A_{ij} are obtained from the A_{ij}^{-1} using the relation $A_{ij}=(-1)^{i+j}A_{ij}^{-1}$, which is due to Haskell (1962).

The R_{st} are Dunkin's (1965) delta matrix elements of the J-matrix. Their definition is

$$R_{st}=J\begin{pmatrix} j & k \\ l & m \end{pmatrix}=J_{jl}J_{km}-J_{jm}J_{kl}$$

where $s=1,2,3,4,5,6$ corresponds to the pairs $jk=12,13,14,23,24,34$ and with the same correspondence of t to lm (see Harkrider (1970)). Or, again in matrix form, one obtains

$$\begin{pmatrix} R_{11}\dot{u}_0/c \\ -R_{11}\dot{w}_0/c \\ 0 \\ 0 \end{pmatrix}=\begin{pmatrix} -R_{11} & 0 & R_{13} & R_{15} \\ 0 & R_{11} & R_{12} & R_{13} \\ 0 & 0 & 0 & 0 \\ 0 & 0 & 0 & 0 \end{pmatrix}A^{-1}\begin{pmatrix} \Delta_1 \\ \Delta_2 \\ \Delta_3 \\ \Delta_4 \end{pmatrix}. \tag{2}$$

Symmetry properties of R_{st} and A_{ij}, like $R_{13}=R_{14}$ or $A_{11}=A_{44}$, are used in obtaining (2).

The surface displacements cannot be computed numerically using (2) for lower phase velocities than the velocities of P- and S-waves due to accuracy problems. These are the same problems, which led Dunkin (1965) to introduce in seismology the delta matrices instead of the Haskell matrices. Červený (1974) has proposed to compute Haskell matrix elements from delta matrix elements in order to improve the accuracy. However, attempts to apply this method to avoid numerical problems did not result in great improvements.

For the case of one layer on top of the half-space where the source is on the bottom of the layer, (2) can be written in this form:

$$R_{11}\dot{u}_0/c=(R_{11}^h\,R_{12}^h\,2R_{13}^h\,R_{15}^h\,R_{16}^h)\begin{pmatrix} -R_{11}^l & 0 & R_{13}^l & R_{15}^l \\ -R_{21}^l & 0 & R_{23}^l & R_{25}^l \\ -R_{31}^l & 0 & R_{33}^l-0.5 & R_{35}^l \\ -R_{51}^l & 0 & R_{53}^l & R_{55}^l \\ -R_{61}^l & 0 & R_{63}^l & R_{65}^l \end{pmatrix}\cdot(A^l)^{-1}\begin{pmatrix} \Delta_1 \\ \Delta_2 \\ \Delta_3 \\ \Delta_4 \end{pmatrix} \tag{3}$$

$$-R_{11}\dot{w}_0/c=(R_{11}^h\,R_{12}^h\,2R_{13}^h\,R_{15}^h\,R_{16}^h)\begin{pmatrix} 0 & R_{11}^l & R_{12}^l & R_{13}^l \\ 0 & R_{21}^l & R_{22}^l & R_{23}^l \\ 0 & R_{31}^l & R_{32}^l & R_{33}^l-0.5 \\ 0 & R_{51}^l & R_{52}^l & R_{53}^l \\ 0 & R_{61}^l & R_{62}^l & R_{63}^l \end{pmatrix}\cdot(A^l)^{-1}\begin{pmatrix} \Delta_1 \\ \Delta_2 \\ \Delta_3 \\ \Delta_4 \end{pmatrix}$$

where h and l stand for half-space and layer, respectively. Watson's (1970) reduced delta matrix extension is used to work with 5×5 matrices instead of 6×6 matrices. Multiplying the two layer matrices first, one obtains

$$R_{11}\,\dot{u}_0/c=(R^h_{11}R^h_{12}R^h_{13}R^h_{15}R^h_{16})\begin{pmatrix}-A^l_{22} & A^l_{12} & 0 & 0\\ -A^l_{32} & 0 & A^l_{12} & 0\\ -A^l_{42} & -A^l_{33} & A^l_{22} & A^l_{12}\\ 0 & -A^l_{42} & 0 & A^l_{22}\\ 0 & 0 & -A^l_{42} & A^l_{32}\end{pmatrix}\begin{pmatrix}\Delta_1\\ \Delta_2\\ \Delta_3\\ \Delta_4\end{pmatrix}$$

$$-R_{11}\,\dot{w}_0/c=(R^h_{11}R^h_{12}R^h_{13}R^h_{15}R^h_{16})\begin{pmatrix}-A^l_{21} & A^l_{11} & 0 & 0\\ -A^l_{31} & 0 & A^l_{11} & 0\\ -A^l_{41} & -A^l_{31} & A^l_{21} & A^l_{11}\\ 0 & -A^l_{41} & 0 & A^l_{21}\\ 0 & 0 & -A^l_{41} & A^l_{31}\end{pmatrix}\begin{pmatrix}\Delta_1\\ \Delta_2\\ \Delta_3\\ \Delta_4\end{pmatrix}. \quad (4)$$

The result of the multiplication of the Haskell layer matrix and the delta layer matrix in (3) is a matrix containing only Haskell elements, and not a new type of elements, as one could expect. If in (4) the Haskell elements for one layer are replaced by elements of the Haskell product matrix of any number of layers, (4) is still true. This was also checked numerically for cases where numerical problems do not appear. In this case the label h means the half space and all layers below the source, and the label l means all layers above the source. Using (4) means doing a (1×5) delta matrix multiplication through the complete model, because R_{11} is needed. When the source level is passed, the elements of the (1×5) product delta matrix must be stored. A (4×4) Haskell matrix multiplication through all layers above the source is also required. Then the first two columns of this Haskell product matrix is used to set up a matrix according to (4). This new matrix is then multiplied with the (1×5) product delta matrix, which contains only layers up the source level. The advantage of using (4) is, that the numerical problems disappeared in all encountered cases. The equations (4) contain much simpler expressions than (2).

Harkrider (1964) has given the displacement-stress source vector for several source types. We will use in the present paper only two of these sources, the vertical single force and the explosive point source. The source vector for the vertical single force is according to Harkrider (1964) $(0,\ 0,\ -\bar{L}(\omega)\,k/(2\pi),0)$, where $\bar{L}$ is the Fourier transformed force-time function and k the wavenumber. If we express the compressional potential of the wave radiated from the explosive point source as $\bar{L}(\omega)\,\exp(-i\,k_\alpha R)/R$, then we obtain for the source vector of the explosive point source, following Harkrider (1964), the expression $(0,\ -2ik^2\,\bar{L}(\omega),\ 0,\ 4ik^2\,\beta_s^2\,\rho_s\,\bar{L}(\omega))$, where i is the imaginary unit and β_s and ρ_s are the shear velocity and density of the source layer, respectively.

Finally Harkrider (1964) arrives for the considered two sources at the following expressions $\bar{u}_0$ and $\bar{w}_0$ for the Fourier transformed surface displacements

$$\bar{u}_0 = -\int_{k_1}^{k_2} \frac{1}{k} \dot{u}_0/c\, J_1(k r)\, dk$$
$$\bar{w}_0 = -i \int_{k_1}^{k_2} \frac{1}{k} \dot{w}_0/c\, J_0(k r)\, dk. \tag{5}$$

Here the integration is already limited to a finite k-window. J_0 and J_1 are the Bessel functions of order zero and one. The asymptotic approximations of the Bessel functions for large arguments for propagation in positive r-direction is used. Since the integration is carried out along the real axis, attentuation is used to shift the poles away from the real axis. The attentuation is determined by the Q-factor for P-and S-Waves in each layer. The Q-factors are used to determine complex velocities (see Schwab and Knopoff (1972)). The integrals (5) are computed numerically using the trapezoidal rule.

A Test of the Method

In order to test the method, the displacements at the surface of the homogeneous half-space was computed for a vertical single force at a depth close to the surface. This problem is very similar to Lamb's problem (Lamb, 1904). The differences are, that in the original form of Lamb's problem the force is acting at the surface of the half-space, and the effects of attenuation are included in the present solution of the problem. A half-space was chosen with a P velocity of 6.0 km/s, and an S velocity of 4.5 km/s, and a density of 2.5 g/cm^3. The attenuation factor Q_α for P waves was 200, and Q_β, the attenuation factor for S waves was chosen to be 4/9 Q_α. The source depth was 1 km. The spectrum $\bar{L}(\omega)$ of the vertical single force $L(t)$ was chosen as follows:

$$\bar{L}(\omega) = \tfrac{1}{2}\left(1 + \cos\frac{\pi\omega}{\omega_0}\right), \qquad -\omega_0 \leqq \omega \leqq \omega_0 \tag{6}$$

where $\omega_0 = 2\pi/T_0$, $T_0 = 1.4$ s (cut-of period). The time function of this spectrum is similar to Lamb's original input signal. The acausality of this input signal is removed by a time shift of half the duration.

In Figure 1 are shown the vertical and horizontal displacements of the Rayleigh wave. The same seismograms are plotted on a 40 times larger amplitude scale in Figure 2, in order to make visible the much smaller P and S waves. The signal forms of all phases are in very good agreement with those obtained by Lamb. Two seismograms from Lamb's paper can be found in Ewing, Jadetzky and Press (1957, Figs. 2–18). The same problem was also computed by Müller and Kind (1976) with similar good results, using a different version of the reflectivity method. There are differences to the seismograms obtained by Lamb in the Figure 1 and 2, which result from the somewhat different model. The amplitudes of the Rayleigh waves decay faster than the inverse square root of the distance, which is due to the attentuation. It is also possible to see in

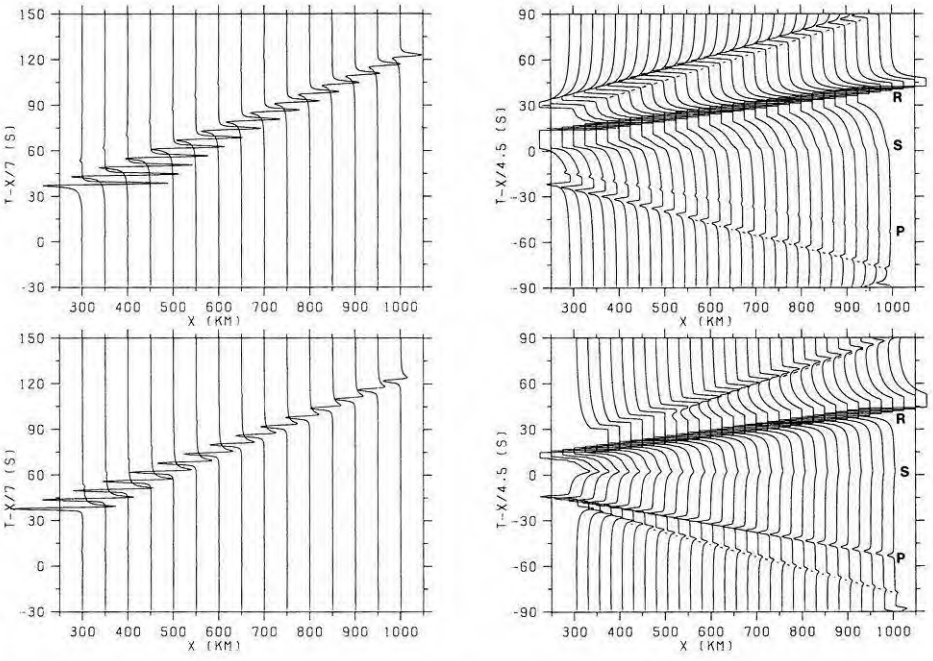

Fig. 1. Theoretical seismograms for Lamb's problem computed with the reflectivity method for a buried source. Top: vertical displacement components (upward motion to the left). Bottom: radial displacement component (motion towards the source to the left). The dominant arrival is the Rayleigh wave

Fig. 2. Same as Figure 1 on a 40 times larger amplitude scale. The Rayleigh wave amplitudes are clipped. Dashed lines mark non-physical phases which are due to the computational method. They are also visible in other figures

Figure 1, that the seismograms at larger distances contain less high frequencies than those at shorter distances, which is also due to the attenuation. Another difference to Lamb's original seismograms can be seen in Figure 2: The sign of the P wave on the horizontal component is reversed. This is due to the location of the receivers at a level above the source, where the first motion of the P wave of the vertical single force is dilation.

Examples

A few examples of computed seismograms will be discussed in this section. The Jeffreys-Bullen earth model was used in all examples. The earth-flattening approximation of Müller (1977) is applied. The P wave attenuation factor Q_α was assumed 50 in the crust, 200 in the uppermost mantle with a gradual increase to 5000 at 800 km depth. The high attenuation in the crust was chosen in order to make the integrand smoother and to save computer time. The choice of Q is no limitation of the method. The S wave attenuation factor was assumed

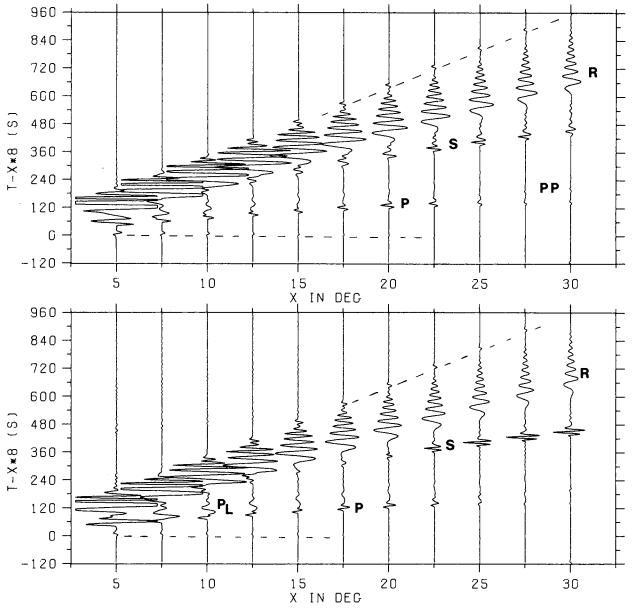

Fig. 3. Vertical (top) and radial (bottom) displacement components due to an explosive source in 300 m depth (Jeffreys-Bullen model). Lower and upper cut-off phase velocities are 2.8 and 15 km/s, respectively, cut-off period is 8.4 s. No amplitude correction due to the earth-flattening approximation is applied in this figure and in Figure 4. The decay of the *P* amplitudes with distance is too fast because the halfspace was assumed at a too shallow depth

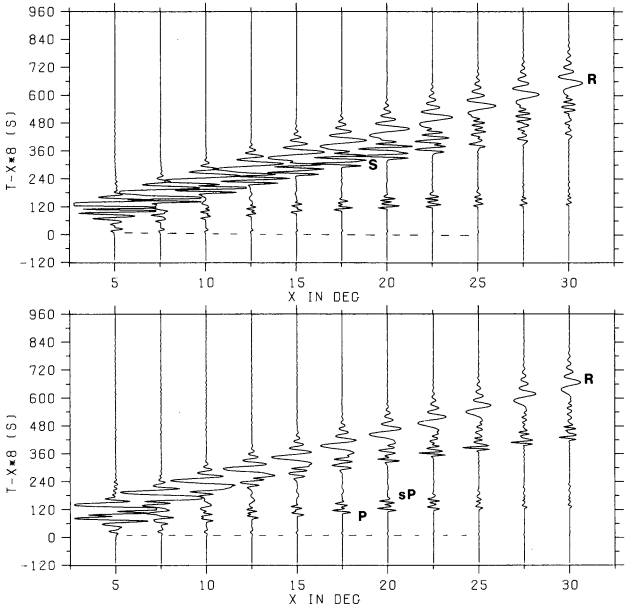

Fig. 4. Vertical (top) and radial (bottom) ground velocity components due to a vertical single force at 100 km depth. All other parameters are identical with those in Figure 3

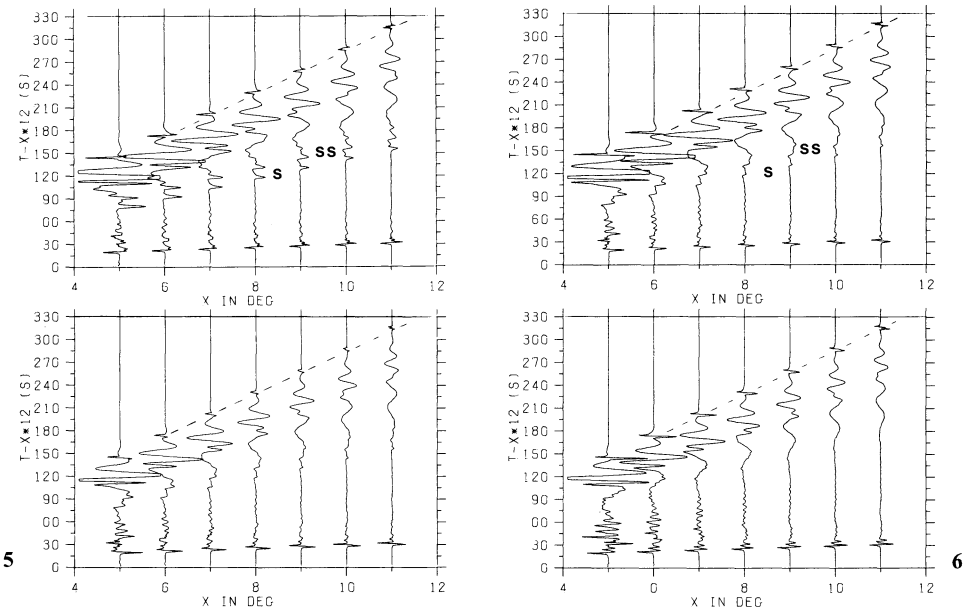

Fig. 5. Vertical (top) and radial (bottom) ground velocity components due to a vertical single force at 300 m depth

Fig. 6. Vertical (top) and radial (bottom) ground displacement components due to an explosive point source at 300 m depth. All other parameters are identical in Figures 5 and 6

to be 4/9 Q_α. Figure 3 shows complete theoretical seismograms for an explosive source in 300 m depth. Equation (6) was chosen as source spectrum with a short period cut-off at $T_0 = 8.4$ s. The dominant phases are P and S and the Rayleigh waves. The Rayleigh waves show clear regular dispersion, shorter periods, which would show inverse dispersion, are not contained in the source signal. P decays very rapidly beyond about 20°, this is due to the assumption of a homogeneous half-space below 800 km depth in the model. Weak indications of PP are visible. The complication of S on the radial component beyond 20° is probably due to interference with shear coupled P_L-modes. Direct P_L-modes are clearly visible, especially on the radial component. In Figure 4 the ground velocity is displayed due to a single vertical force at a depth of 100 km. All other parameters are identical with those of Figure 3. The dominant phases are essentially the same in Figure 4. The Rayleigh waves are less well developed than in Figure 3, as it is expected for a source at depth. Depth phases appear clearly on both components.

Next the Figure 5 and 6 will be discussed. All parameters are kept identical in both figures, except that the source in Figure 5 is a vertical single force, and in Figure 6 an explosive source. Source depth is 300 m, cut-off period is 1.6 s. The phase-velocity window is from 11 to 2.75 km/s. Figure 5 cannot be compared directly with recordings of nuclear explosions, because of differences in the

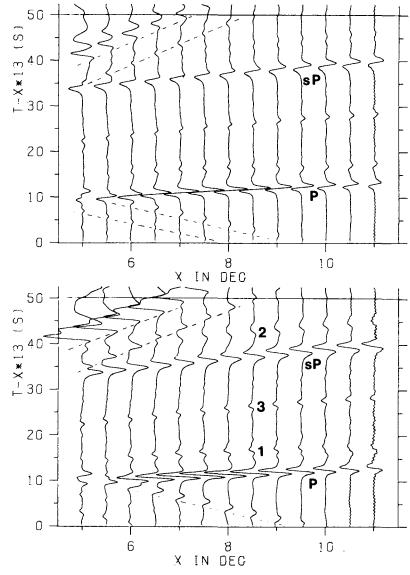

Fig. 7. Vertical (top) and radial (bottom) ground displacement due to a vertical single force at 100 km depth. Major phases are *P* and *sP*. The weaker phases are due to conversions and reflections at the Moho. See text for more details

source spectra. A nuclear explosion is radiating less energy at long periods, whereas the source function (6), which is also used in Figure 5 and 6, is more earthquake-like. The dominant phases are the same as in the previous figures. Because of the higher resolution in Figures 5 and 6, the phases *S* and *SS* are separated. As it is expected, the seismograms of the two figures, are very similar, except that the seismograms of the single force contain more *S* energy.

The reflectivity method can easily be used for the computation of individual phases alone. For example, if one is only interested in *P* waves, then one should choose the proper integration window for that purpose. Figure 7 shows an example for the *P* waves from a vertical single force at 100 km depth. The cut-off period is 0.6 s, the limits of the integration are 6.4 and 10.5 km/s. The dominant phases in Figure 7 are *P* and *sP*. In addition, a number of weaker phases can be recognized on both components. These phases are all due to converted and reflected waves at the crust-mantle boundary. For example, two weak phases, labelled 1 and 2, can be recognized, especially on the horizontal component, about 5 s after *P* and *sP*, respectively. These phases are probably *S* waves, generated at the Moho by the two larger *P* phases in front. Another weak phase inbetween *P* and *sP*, labelled 3, is probably an *sP* phase, which is reflected at the Moho instead the free surface.

Conclusions

The present extension of the reflectivity method in connection with an earthflattening approximation allows to compute the complete response of a vertically inhomogeneous earth, as far as the earth-flattening approximation can be used.

The location of the source is arbitrary. It is also a method which can easily be adopted to special problems by choosing the proper wavenumber window. A limitation of the method is probably its long computation time.

Acknowledgments. This research was supported by a grant of the Deutsche Forschungsgemeinschaft. Parts of the computations have been carried out at the computer center of the university of Karlsruhe. I wish to thank Vladislav Červený and Gerhard Müller for discussions and suggestions, and Gerhard Müller for reading the manuscript.

References

Červený, V.: Reflection and transmission coefficients for transition layers. Studia geophys. geodaet. **18**, 59–68, 1974

Dunkin, J.W.: Computation of modal solutions in layered media at high frequencies. Bull. Seism. Soc. Am. **55** (2), 335–358, 1965

Ewing, W.M., Jadetzky, W.S. and Press, F.: Elastic waves in layered media, New York: McGraw-Hill, 1957

Fuchs, K.: The reflection of spherical waves from transition zones with arbitrary depth-dependent elastic moduli and density. J. Phys. Earth **16**, Special Issue, 27–41, 1968

Harkrider, D.G.: Surface waves in multilayered elastic media, 1. Rayleigh and Love waves from buried sources in a multilayered elastic halfspace. Bull. Seism. Soc. Am. **54**, 627–679, 1964

Harkrider, D.G.: Surface waves in multilayered elastic media. Part II. Higher modes spectra and spectral ratios from point sources in plane layered earth models. Bull. Seism. Soc. Am. **60**, 1937–1987, 1970

Haskell, N.A.: Dispersion of surface waves on multilayered media. Bull. Seism. Soc. Am. **43**, 17–34, 1953

Haskell, N.A.: Crustal reflection of plane *P* ans *SV* waves, J. Geophys. Res. **67**, 4751–4767, 1962.

Lamb, H.: On the propagation of tremors over the surface of an elastic solid. Phil. Trans. R. Soc. (London) A, **203**, 1–42, 1904

Müller, G.: Earth-flattening approximation for body waves derived from geometric ray theory – improvements, corrections and range of applicability. J. Geophys. **42**, 429–436, 1977

Müller, G., Kind, R.: Observed and computed seismogram sections for the whole earth, Geophys. J.R. astr. Soc., **44**, 699–716, 1976

Schwab, F.A., Knopoff, L.: Fast surface wave and free mode computations. Methods in computational physics, Vol. II, B.A. Bolt, ed. New York: Academic Press 1972

Watson, T.H.: Fast computation of Rayleigh wave dispersion in a layered halfspace. Bull. Seism. Soc. Am. **60**, 161–166, 1970

Received April 24, 1978 / Revised version June 29, 1978